

## Controlled Release Formulation of Dichlorvos and Diazinon Using Biocompatible Starch For Agro-Environment Sustainability

<sup>1</sup>Okafor E.C., <sup>2</sup>Okonkwo S.I., <sup>3</sup>Okafor Ifeoma and <sup>4</sup>Odinma S.C.

<sup>1</sup>Department of pure and industrial chemistry, Nnamdi Azikiwe University Awka, Nigeria

<sup>2</sup>Department of pure and industrial chemistry, Chukwuemeka Odumegwu Ojukwu University Uli, Nigeria

<sup>3</sup>National agency for food and drug administration and control, Nigeria

<sup>4</sup>Department of Industrial Chemistry, Caritas University Amorji Nike Enugu Nigeria

---

### Abstract

The study was carried out with the aim of encapsulating suitable and sustainable controlled release micro formulation of dichlorvos and diazinon; organophosphate pollutant used as a pesticide for agriculture in Nigeria with low cost adsorption of the insecticides; dichlorvos and diazinon matrix. The maximum absorbance of dichlorvos derivative and diazinon were measured at the wavelength of 401 nm and 265 nm respectively. Langmuir and Freundlich adsorption isotherms fitted the adsorption data generated at pH 4.0, 7.0, 9.0 and 25°C for the different surfaces. Langmuir and Freundlich adsorption isotherm were used to model the adsorption process. Controlled release formulations (CRFs) were synthesized from sodium alginate-modified starch matrix and cross-linked with 0.25M CaCl<sub>2</sub> solution. Fourier transform infrared (FTIR) spectroscopy, scanning electron microscopy (SEM), and powder X-Ray diffractometry (PXRD), were used to characterize the CRFs.

**Keywords:** adsorption, starch, CRFs, dichlorvos and diazinon

---

Date of Submission: 03-06-2021

Date of Acceptance: 17-06-2021

---

### I. Introduction

The vast majority of the world's hungry people live in developing countries where 12.9% of the population is undernourished [7]. The economy of third world countries is centred mainly on agriculture, whose output has continued to lag behind the world's food demands [12]. Pesticide formulation which are mostly used by farmers, reduce labour costs and energy consumption and in so doing, increase labour efficiency and food production [2]. Most of the commonly used pesticides are classified, using empirical toxicological data, as endocrine disruptors, carcinogens and nerve toxins. Parenthetically, interactive drawback associated with conventional formulations of pesticides presently in use, is the release of much of their active ingredients into the immediate environment, which results in significant loss of the active ingredient in the field via the dissipation pathways of hydrolysis, volatilization, evaporation, and leaching. A consequence of this loss is their repeated and often excessive application in farm plots or field situation. It has been estimated that 90% of applied pesticides do not reach their target areas at the right time and in efficacious quantities [18]. Thus, in addition to toxicity problems, conventional methods of pesticide application impact negatively on the economics of food and fibre production.

The search for more efficient methods and processes which afford higher yields and a better quality that require less time, money, methods and processes, and do not pose a threat to the environment, has received an impetus with the recent adoption of the Sustainable Development Goals (SDGs) as the current global development paradigm for the period 2015 - 2030 [14,33]. This formulation is a recent strategy, borrowed from the drug industry, that releases the chemicals slowly, in a controlled and sustained manner and are such called slow or controlled release formulations (SRFs or CRFs) [28,4]. The formulation and optimization of biodegradable, biocompatible pesticide-laden matrix as delivery systems provide answers to the problems associated with pesticide use in food and fibre production as outlined above.

Dichlorvos and diazinon as shown in Fig. 1 are broad spectra organophosphate insecticide. They are used in agriculture and horticulture for the control of insects in crops, ornamentals, lawns, fruit and vegetables and as pesticides in homes and public buildings. As a result of their wide usage and application by conventional methods, its residues are usually found in food crops, natural water systems and in soils [34]. Therefore, there is need for CRFs of the both insecticide types which are cleaner and safer for the user, having minimal impact on the environment and are applied at the lowest dose rate [20,5]

---

This research is set out to encapsulate dichlorvos and diazinon, the active ingredient (a.i.) into starch cross-linked with sodium alginate. Starch attracts considerable attention as a polymeric material for CR because, apart from it being renewable, abundant, and inexpensive, it can be easily modified chemically, physically and biologically into low molecular weight or high molecular weight compounds for specific applications [6,21]. It is a non toxic, biodegradable and biocompatible [30] matrix, whose CRFs enhances easy application by farmers and minimise direct contact with the environment.

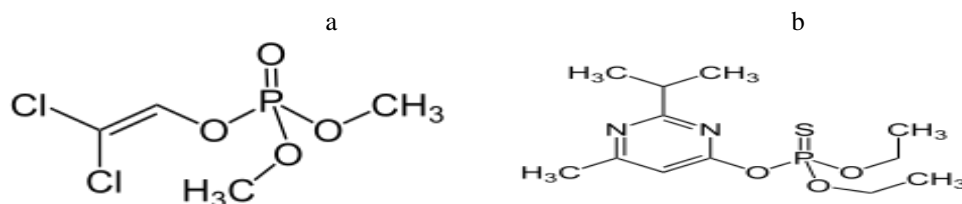


Fig. 1: (a) dichlorvos and (b) diazinon

## II. Materials and Methods

### 2.1. Materials

Dichlorvos (DDPV), diazinon both are technical grades and sodium alginate were acquired from Zayo Sigma Jos, Nigeria. Phthalate buffer pH 4.0 solution, potassium dihydrogen phosphate, acetone, sodium hydroxide, glacial acetic acid, calcium chloride, sodium chloride, ninhydrin, dimethyl sulphide (DMSO) were all supplied by NAFDAC Zonal Laboratory, Agulu, Nigeria. and chemicals were used as received.

### 2.2 Preparation of stock solutions for calibration experiments

#### 2.2.1 Dichlorvos and diazinon

A stock solution of dichlorvos and diazinon of 1000 µg/ml was prepared by dissolving 0.045 mmol of dichlorvos in acetone and made up to 100 ml mark with milli-Q water. The volumes of the stock solution were measured into 10 ml volumetric flasks using an Eppendorf pipette to obtain solutions whose corresponding concentrations range between 10.0 - 30.0 µg/ml, after making up to the mark with milli-Q water.

#### 2.2.2 Preparation of ninhydrin-dichlorvos reagent for calibration curve

1 ml dichlorvos sample solution was added into 2 ml of the ninhydrin reagent in a plastic screw-capped bottle. The ninhydrin reagent was prepared by adding 30 ml of DMSO into a conical flask containing 1.4 mmol ninhydrin with stirring, 0.043 ascorbic acid was added with further stirring for another 3 minutes to ensure complete dissolution [19].

### 2.3 Preparation of controlled release formulations (CRFS)

A 3% (w/w) aqueous dispersion containing of sodium alginate in 100 ml of water, 2% (w/v) of the pesticide (0.02 g in 1ml of acetone) and 15% (w/w) of each matrix was vigorously stirred for 10 minutes. The CR beads were formed by dripping the slurry from a 500 ml syringe from a height of approximately 20 cm into excess 200 ml gelling solution made up of 0.25M CaCl<sub>2</sub>·2H<sub>2</sub>O in 2% v/v acetic acid at 25<sup>o</sup>C. The beads, which were allowed to set for 25 minutes, were filtered using a funnel, washed twice with Milli-Q water and air-dried. Blank beads were prepared in the same way but without any active ingredient.

### 2.4 characteristics of the insecticides-loaded beads using fourier transforms infra-red (FTIR) and powder x-ray diffraction (PXRD)

The FTIR spectra were obtained for the pulverized samples of blank starch and a.i.-incorporated CRFs, using a Thermo-nicolet 380IR, USA FTIR spectrophotometer. The samples were scanned within the range 400-4000 cm<sup>-1</sup> at a resolution of 2 cm<sup>-1</sup>. In PXRD analysis, the prepared insecticidal controlled release starch formulations of dichlorvos and diazinon were structurally analyzed using the diffractometer, (INEL Equinox 1000g/N USA). The samples were first sieved onto the surface of a silicon disc pre-coated with petroleum jelly, and then scanned from 0-140<sup>o</sup> (2θ) at the speed of 5/min.

### 2.5. Scanning electron microscopy (SEM)

SEM images of the CRF samples were recorded using a Tecnai 920, USA scanning electron microscope, equipped with energy dispersive analysis of X-rays (EDAX) at the required magnification. The acceleration voltage used for the SEM instrument was 10 keV with the secondary electron image (SEI) as a detector.

## 2.6. Studies of adsorption equilibria

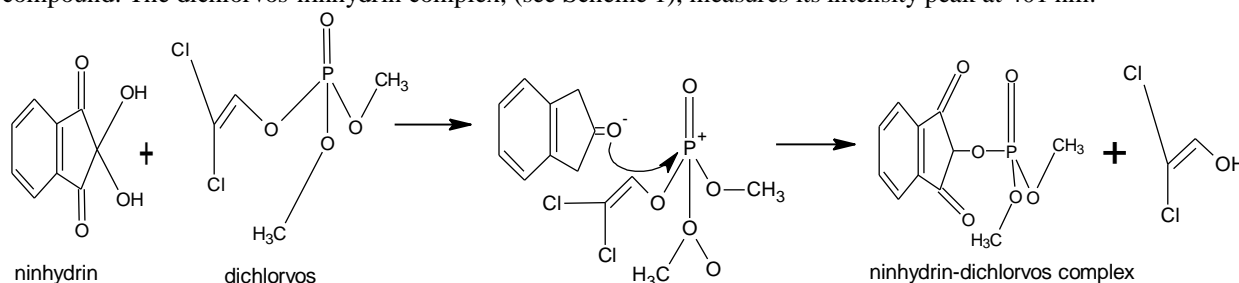
Adsorption equilibrium studies involving the pesticides of interest were undertaken, using the batch equilibration method [26, 24]. 10 ml of the buffer solutions (pH 4, 7 and 9) and 40 ml of diazinon and dichlorvos solutions were introduced into a Teflon bottle containing 250 mg of the adsorbent, respectively. The samples were thoroughly shaken on a mechanical shaker for 1 hour at the temperature 25°C. The suspension was subsequently centrifuged (Megafuge, Heraeus) at 4500 rpm for 10 minutes. Five ml of the supernatant was withdrawn for UV-Vis spectrophotometry (Shimadzu Japan) analysis of the active ingredient at the wavelength of 401 and 264 nm for dichlorvos and diazinon, respectively. Each experiment was duplicated. Pesticide solutions in buffer without the adsorbent were also treated in similar manner to serve as blank. The amount of adsorbed dichlorvos and diazinon at equilibrium  $q_e$  (mg/g) were calculated by principle of mass balance (equation 1) [25]: where  $C_o$  and  $C_e$  are initial and final equilibrium concentrations (mg/l) of the pesticide in the aqueous phase, respectively, with  $V$  = volume of aqueous solution taken in litres and  $W$  = mass of adsorbent in grams. The Gibbs free energy values for  $\Delta G_{ads}^L$  and  $\Delta G_{ads}^F$  (kJmol<sup>-1</sup>) were calculated with the application of equation 2 while the Langmuir adsorption constant;  $K_L$  (mg/g),  $b_L$  (L/mg) and  $R_L$  and Freundlich adsorption constants;  $K_F$  and  $n$  were obtained using equations 3 and 4.

$$q_e = (C_o - C_e) \times \frac{V}{W}$$

## III. Result And Discussion

### 3.1 Quantification of the pesticides, dichlorvos and diazinon

Diazinon has its maximum wavelength at 264 nm. Dichlorvos was first derivatised with ninhydrin because the molecule does not absorb light in the 200–800 nm [31] for direct spectrophotometric quantification of the compound. The dichlorvos-ninhydrin complex, (see Scheme 1), measures its intensity peak at 401 nm.



**Scheme 1:** A possible reaction of ninhydrin with 2,2-dichlorovinyl dimethyl phosphate (dichlorvos) to form dimethyl phosphate-ninhydrin complex

### 3.2 Physicochemical and morphological characterization of starch CRFs of dichlorvos and diazinon

#### 3.2.1 FTIR of starch CRFs of dichlorvos and diazinon

The FTIR spectra of blank starch, dichlorvos- and diazinon-loaded starch are shown in Figs. 2a-c; the spectral assignments are summarized in Table 1. In the blank starch spectrum (Fig. 2a), the broad band resulting from the stretching vibration of hydroxy group (O-H) appears at the 3418 cm<sup>-1</sup> (Shi *et al.* 2019). The sharp strong peak at 2931 cm<sup>-1</sup> is characteristic of the C-H stretching vibration of methylene group [13,8,32]. The two prominent absorption bands at 1639 cm<sup>-1</sup> and 1420 cm<sup>-1</sup> are due to the asymmetric and symmetric stretching vibration of carboxylate (-COO) group in the alginate moiety [8] while the peaks observed at 1156 cm<sup>-1</sup> and 1020 cm<sup>-1</sup> are assigned to C-O-C bond stretching in polysaccharides [8]. The FTIR spectrum of dichlorvos-loaded starch matrix shows peaks in the region of 708 – 577 cm<sup>-1</sup> for the stretching vibration band of chloro-alkanes (C-Cl), a functional group in the active ingredient, dichlorvos [29]. It is seen that the peaks centred at 3418 and 2931 cm<sup>-1</sup> in the Fig. 2a have broadened and have been shifted in the spectrum of dichlorvos-loaded starch as observed in Fig. 2b to appear at 3432 - 3388 and 2925 cm<sup>-1</sup>. There is a slight broadening of the broad absorption centred at 3416 cm<sup>-1</sup> and 2150 cm<sup>-1</sup> and a reduction in the intensity of the bands at 1154 - 1019 cm<sup>-1</sup> in diazinon-loaded starch (see Fig 2c), when compared with the blank in Fig. 2a. The peaks at 1640 cm<sup>-1</sup> corresponds to the asymmetric vibration of carboxylate -COO<sup>-</sup> in alginate with overlap in the same region as the aromatic ring C-H stretching vibration in diazinon. These changes in the spectra of dichlorvos and diazinon signify interactions between the matrix and the incorporated a.i. Similar results were reported by [12,23,3].

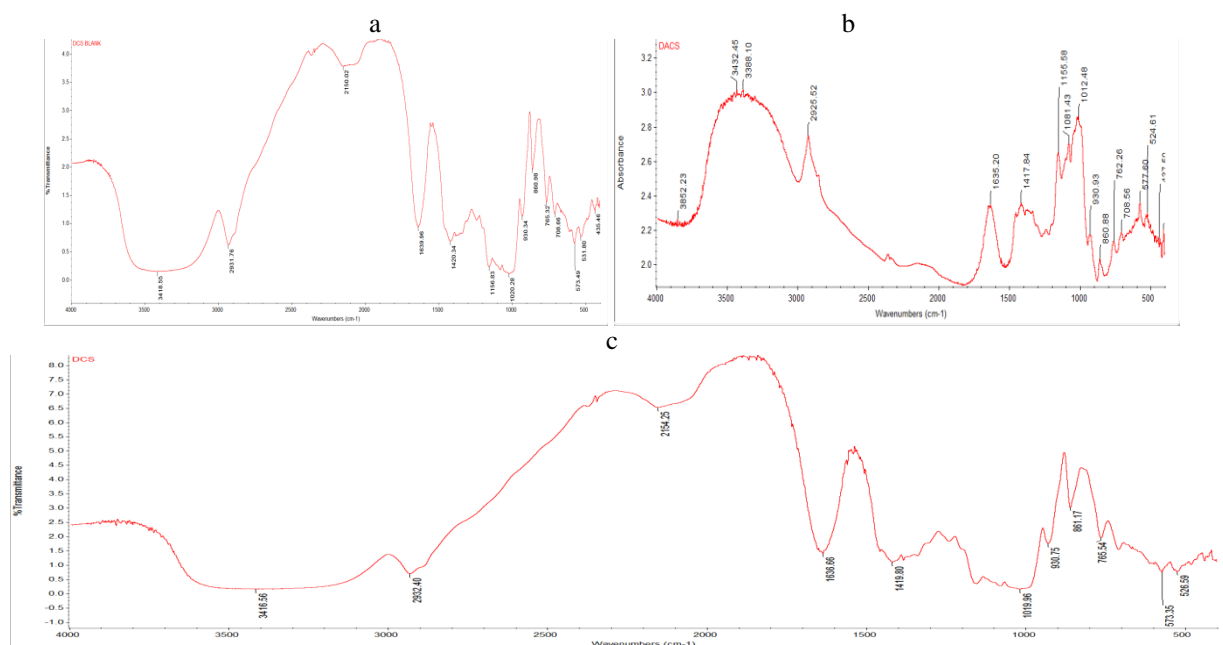


Fig. 2: FTIR spectra of: (a). blank starch, (b) dichlorvos-loaded starch and (c) diazinon-loaded starch

Spectrum	Observed wave number (cm <sup>-1</sup> ) in blank matrices	Observed wave number (cm <sup>-1</sup> ) in dichlorvos loaded- matrices	Observed wave number (cm <sup>-1</sup> ) in diazinon loaded- matrices	Functional group
Starch	3418 2931 1639, 1420  1156- 1020 - - -	3432-3388 2925 1635, 1417  1155-1012 1081 - 930, 860 708- 577	3416 2932, 2150 1646  1154- 1019 - 930 708 -	O-H -CH <sub>3</sub> Asymmetric and symmetric C=O (carboxylate) C – O – C P=O P=S P – O – R C-Cl

Table 1:Major absorption bands and vibrations in FTIR spectra observed in starch, dichlorvos- and diazinon-loaded starch

### 3.2.2 PXRD of starch CRFs of dichlorvos and diazinon

Fig. 4a is the X-Ray pattern of blank starch cross-linked with sodium alginate used as the control. The diffractogram of the blank starch shows significant peaks at  $2\theta^\circ$ . The signals at  $2\theta^\circ = 28^\circ$  and  $45^\circ$  are ascribed to sodium alginate. Nnamonuet *al.*(2012) reported that the XRD of an alginate showed two peaks at  $2\theta^\circ = 38^\circ$  and  $44.5^\circ$  in their sorption studies of trifluralin on alginate modified starch, while Fonteset *al.* (2013) opined that the peaks at  $2\theta^\circ = 13.7^\circ$ ,  $23^\circ$  and  $40^\circ$  were due to alginate in their XRD study of benzathine penicillin G-loaded alginate-starch. The broad peak at  $2\theta^\circ = 25^\circ$  is ascribed to starch in the formulation which is consistent with the result of Jyothiet *al.* (2018) who observed the peaks of natural cassava starch at  $23^\circ$ . The x-ray diffractogram of dichlorvos-loaded starch given in Fig. 4b reveals broader peaks at  $2\theta^\circ = 24^\circ - 28^\circ$  and  $48^\circ - 55^\circ$  when compared with the Fig. 4a (control). Addition of dichlorvos into starch modifies the peaks of the starch matrix from sharp strong peaks to wide broad peaks, which shows that the crystalline structure of the dichlorvos-loaded starch is more amorphous than that of the control. The PXRD spectrum of diazinon-loaded starch (Fig. 4c) showed no evidence of formation of new peaks when compared with that of the blank starch. However, the peaks at  $2\theta^\circ = 24^\circ$ ,  $28^\circ$  and  $48^\circ - 54^\circ$  decreased in intensity in all the diazinon-loaded starch beads. This decrease in the intensity of peaks in diazinon-loaded S100 matrix when compared with the peaks of the control is good evidence for interactions between the matrix and the active ingredient. The changes in the intensity of the bands signify interactions between the starch matrix and dichlorvos/diazinon.

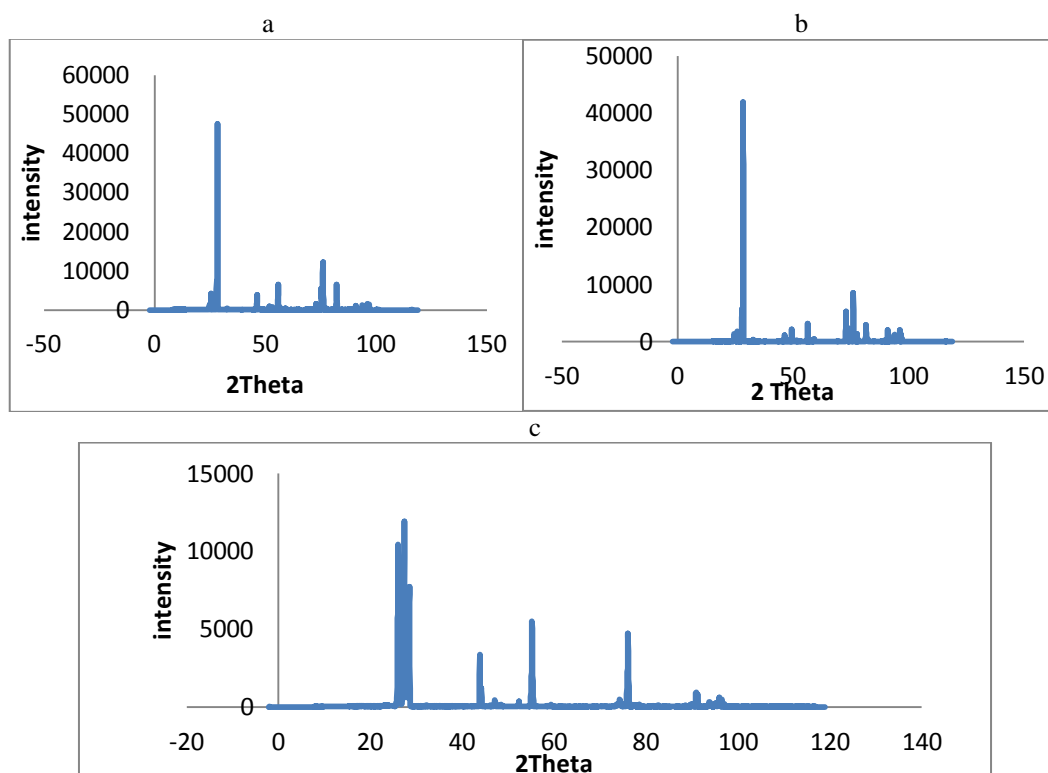
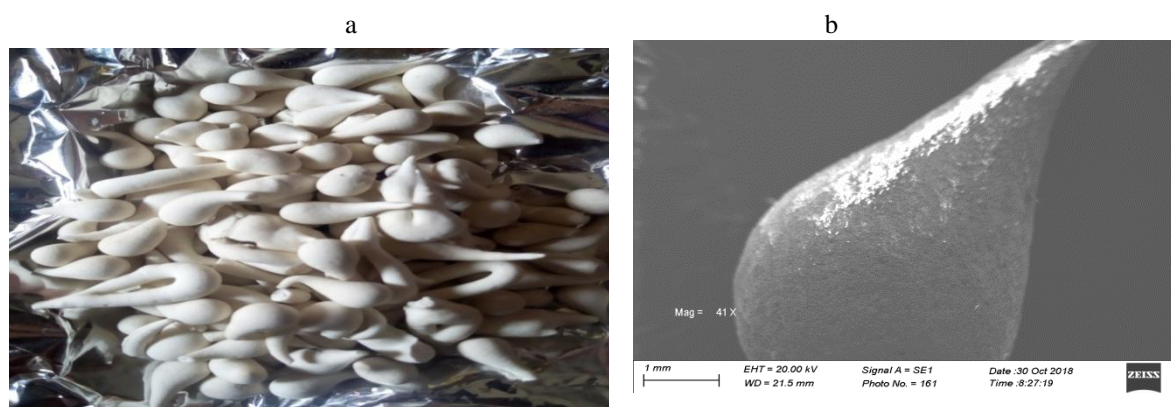


Fig. 4: PXRD spectra of: (a) blank starch (b) dichlorvos-loaded starch and (c) diazinon-loaded starch

### 3.3 Scanning electron microscopy

The real photograph and the SEM microgram of starch beads displayed in Figs. 3a and 3b are spherical in shape with a protruded edge, and have smooth surfaces [29]. The dichlorvos- and diazinon-loaded starch formulation given in Figs. 3c and 3d had similar cross-sectional morphology which shows moderately dense structure, big round holes and a distribution of unequal micro pores across the surface [17]. The internal structure of dichlorvos-loaded starch (see Fig. 3e) is a spatial, smooth, spherical mass of porous particles and the diazinon-loaded starch presented in Fig. 3f displays segregated, heterogeneous large lumps with cracks and crevices surface [1]. It is conceivable, that the segregated materials, crevices, cracks, spatial and micro-pores seen in the SEM micrograph of the starch CRFs in Figs. 3b - 3f are the channels for dichlorvos and diazinon molecules to diffuse easily in contact with water.



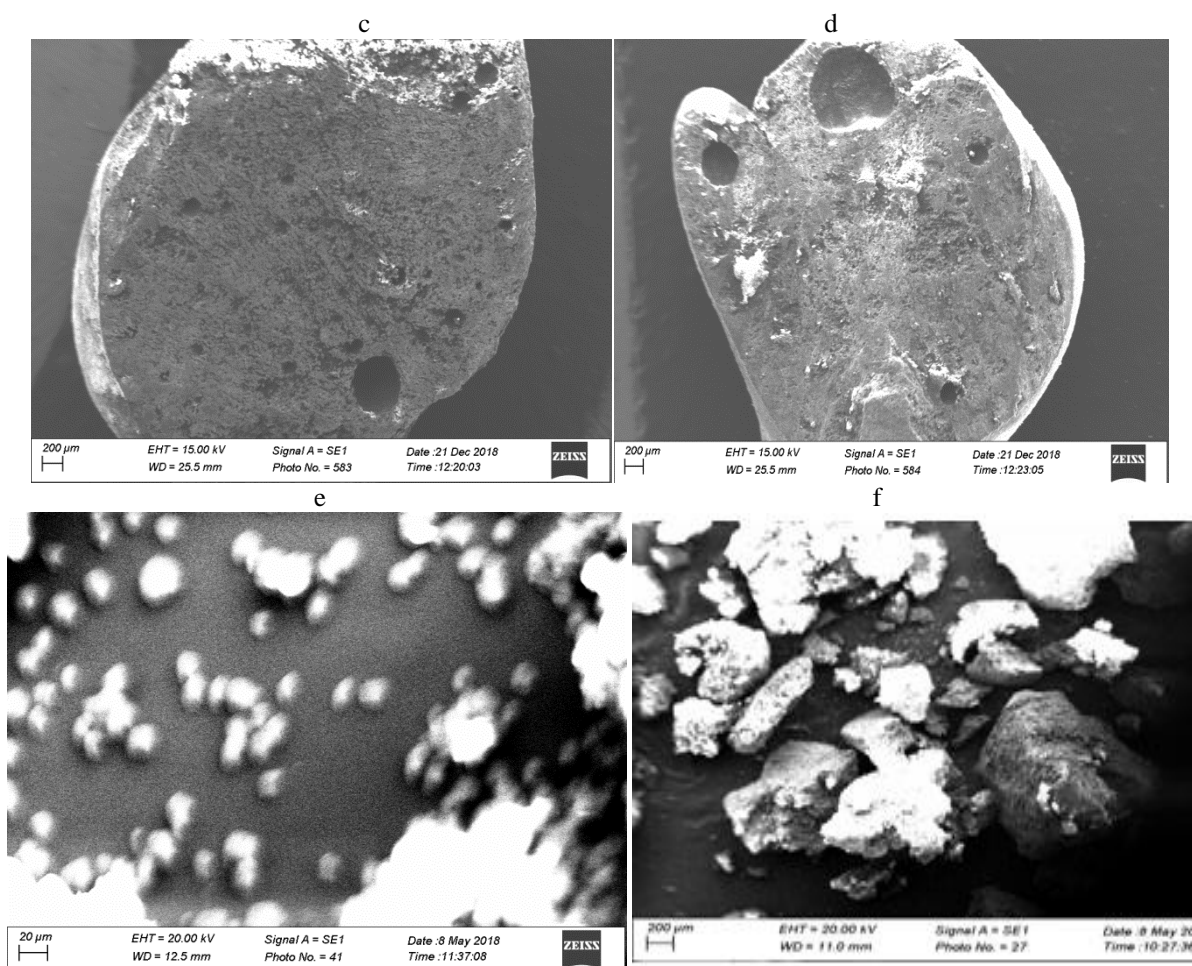


Fig. 3: (a) Photograph of starch beads and SEM micrograph showing (b) external morphology starch; (c) cross-section of dichlorvos-loaded starch and d diazinon-loaded starch; (e) internal morphology of dichlorvos-loaded starch and (f) diazinon-loaded starch.

### 3.4 ADSORPTION ISOTHERM

#### 3.4.1 Langmuir and Freundlich Models

The parameters from the Langmuir and Freundlich isotherms for the adsorption of dichlorvos and diazinon on the starch surfaces are assembled in Tables 2 and 3; these parameters were extracted from the plots of  $\frac{1}{q_e}$  against  $\frac{1}{C_e}$ , and  $\log q_e$  versus  $\log C_e$  stated in equations 3 and 4 for Langmuir and Freundlich, respectively. The correlation coefficients,  $R^2$ , for the Langmuir isotherms for dichlorvos and diazinon adsorption are better than those for Freundlich isotherm. Furthermore, the  $\Delta G_{ads}^o$  values obtained from the Freundlich correlation are lower than the  $\Delta G_{ads}^o$  values usually obtained for the formation of chemical bonds as adsorptive linkage by several orders of magnitude (see table 3). The  $\Delta G_{ads}^F$  values for chemisorption processes typically range from -80 to -400  $\text{kJ mol}^{-1}$  [11] while the  $\Delta G_{ads}^F$  values obtained in this study range from 2.62 - 3.99  $\text{kJ mol}^{-1}$  and 0.20 - 0.24  $\text{kJ mol}^{-1}$  for dichlorvos and diazinon respectively. This provides conclusive evidence that the Freundlich isotherm is not the applicable isotherm to the system under discussion, which supports the ideas of the Langmuir isotherm as the operational model for the adsorption of dichlorvos and diazinon on the starch surface. A similar conclusion was reached by Binhet *al.* (2019) for the adsorption of dichlorvos on coconut fibre biowastes. The  $K_L(\text{mg/g})$  values in Table 2 shows that dichlorvos and diazinon adsorption are pH-dependent, according to the order  $\text{pH } 4 > \text{pH } 9 > \text{pH } 7$ .

Formation of strong hydrogen bonds at pH 4, [10,14] is being responsible for better adsorption of diazinon as presented in Scheme 2 and Fig. 5. This cannot be employed to explain better adsorption of dichlorvos at this pH 4 than in neutral and basic pH. The marginal difference in pHs in the Langmuir adsorption of diazinon onto starch surface may be attributed to the  $\text{pK}_a$  of diazinon = 2.4 [14] as it also influences the protonation of diazinon in pH 4 solution. As the lowest pH of this study is pH 4, the protonated diazinon may have decreased since the  $\text{pK}_a$  value of diazinon is 2.4 [15]. Under the this condition, weak hydrogen interaction may occur between the O-H moiety present in the polymeric starch matrix and the P = S, bonds in diazinon

functional group as shown in Scheme 2 and Fig. 5. However, Gal *et al.* (1992) and Ku *et al.* (1998) observed that hydrogen bond on diazinon occurs at the sulphur region because the sulphur atom is more likely to hold a surrounding with higher electron density than the nitrogen atom on the diazine ring. Tiwari and Bind (2014) measure maximum adsorption at pH 4 in the removal of dichlorvos by super paramagnetic poly(styrene-co-acrylic acid) from water.

The separation factor,  $R_L$ , obtained using equation 5, ranges from 0.056 – 0.758; on the basis of the criteria presented in Table 4, this means that the adsorption of dichlorvos and diazinon on the starch surface are favourable since  $R_L < 1$ . The  $b_L$  (L/mg) values, which relate to the affinity of the binding site, are typically low. The low values of  $b_L$  (L/mg) obtained show that the adsorption of both insecticide types on the starch matrix involve low energies of adsorption which is consistent with the low magnitude of  $\Delta G_{ads}^L$  displayed in Table 2.

$\Delta G_{ads}^L$  (kJ mol<sup>-1</sup>) values for the adsorption of dichlorvos and diazinon onto the matrix at different pH values presented in Table 3 are all negative and small in magnitude, consistent with a spontaneous adsorption process that forms a monolayer of adsorbent held together by weak physical forces. The Gibbs free energy values for  $\Delta G_{ads}^L$  and  $\Delta G_{ads}^F$  kJmol<sup>-1</sup> were calculated with the application of equation 2. The value of  $\Delta G_{ads}^0 = -4.57$  kJ mol<sup>-1</sup> at 298K measured by [3] for the adsorption of dichlorvos on coconut fibre is of the same magnitude as those obtained in this study.

$$\Delta G_{ads}^0 = -RT \ln K$$

2

$$\frac{1}{q_e} = \frac{1}{K_L} + \left(\frac{1}{K_L b}\right) \left(\frac{1}{C_e}\right)$$

3

$$\log q_e = \log K_F + \frac{1}{n} \log C_e$$

4

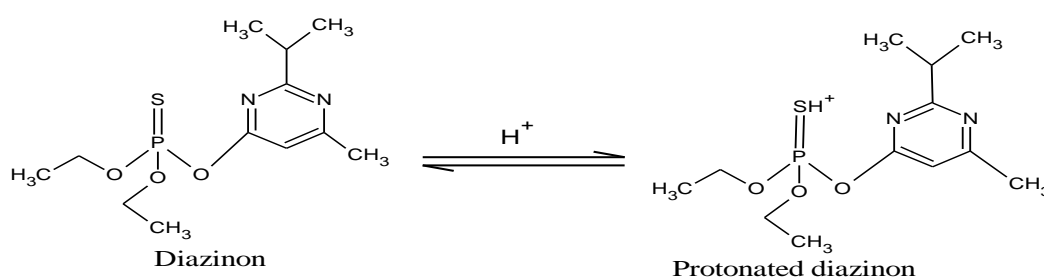
where  $K_L$  is the Langmuir adsorption constant (mg/g);  $C_e$  = equilibrium concentration of a.i. (mg/l) in the aqueous phase;  $q_e$  = amount of a.i adsorbed per unit mass of adsorbent (mg/g); while  $b$  is the Langmuir constant which is a measure of the energy of adsorption. The  $K_F$  is the Freundlich adsorption capacity (mg/g), while  $n$  is the adsorption intensity. When  $n < 1$ , the surface of the adsorbent is heterogeneous in nature.

**Table 2:** Langmuir isotherm parameters for the adsorption of dichlorvos and diazinon on cow dung matrices at 298K

a.i.	Surface	$K_L$	$b$	$R_L$	$R^2$	$\Delta G_{ads}^L$ kJmol <sup>-1</sup>
dichlorvos	pH 4 CD100	5.405	0.025	0.758	0.982	-4.17
	pH 7 CD100	2.222	0.099	0.249	0.997	-1.97
	pH 9 CD100	2.874	0.329	0.387	0.999	-2.61
diazinon	pH 4 CD100	2.755	0.123	0.391	0.988	-2.50
	pH 7 CD100	1.669	0.162	0.328	0.996	-1.27
	pH 9 CD100	1.672	0.179	0.306	0.993	-1.27

**Table 3:** Freundlich isotherm parameters for the adsorption of dichlorvos and diazinon on cow-dung matrices at 298K

	Surface	$K_F$	$n_F$	$R^2$	$\Delta G_{ads}^F$ kJmol <sup>-1</sup>
dichlorvos	pH 4 CD100	5.023	3.597	0.926	-3.99
	pH7 CD100	2.891	0.794	0.984	-2.62
	pH 9 CD100	2.977	5.605	0.854	-2.70
diazinon	pH4 CD100	1.084	2.591	0.907	-0.20
	pH 7 CD100	1.083	2.381	0.959	-0.20
	pH9 CD100	1.101	2.075	0.953	-0.24



Scheme 2: Protonation of the diazinon at pH 4

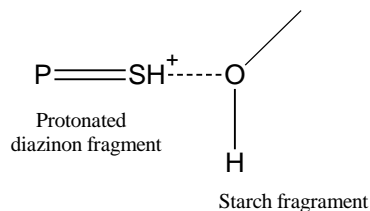


Fig. 5: Possible hydrogen bonding involving hydroxy group in starch fragments in CRFs and the protonated diazinon

$$R_L = \frac{1}{1+bc_0} \quad 5$$

Table 4: the Langmuir separation factor,  $R_L$  (Ngahet *al.* 2004)

Value $R_L$	Meaning
$R_L = 0$	Irreversible
$0 < R_L < 1$	Favourable
$R_L = 1$	Linear
$R_L > 1$	Unfavourable

#### IV. Conclusion

Controlled release beads encapsulating dichlorvos and diazinon, were formulated, using starch matrix, cross linked with alginate and  $\text{CaCl}_2$ . FTIR analysis of the CRFs, showed that there is interactions between the matrix and the incorporated insecticides. The changes observed in the PXRD peaks in the both insecticides-loaded starch beads decrease in the crystallinity nature of the starch beads.  $\Delta G_{ads}^0$  values derived from  $K_L$  and  $K_F$ , have small magnitude and are all negative, describing the adsorption process as physisorption type and spontaneous. The maximum adsorption of dichlorvos and diazinon on starch matrix were recorded at pH 4.

#### Reference

- [1]. Adriano, V.R., Marcos, R.G., Thais, A.M., Luiz, H.M.C., Edvani, C.M., Elias, B.T. (2008). Synthesis and characterization of a starch-modified hydrogel as potential carrier for drug delivery system. *Journal of Polymer Science: Polymer chemistry*. Volume 46, Issue 7, 1 April 2008, Pages 2567 – 2574.
- [2]. APVMA, (2008): Australian pesticide and veterinary medicine authority (2005) Dichlorvos Environmental assessment APVMA P.O Box, E240 Kingston Act 2604 Australia pg 1-71.
- [3]. Binh, Q.A., Tungtakanpoung, D. and Kajitvichyanukul, P. (2019): Similarities and differences in adsorption mechanism of dichlorvos and pymetrozine insecticides with coconut fiberbiowaste sorbent, *Journal of Environmental Science and Health, Part B*.
- [4]. Campos, E.V., de Oliveira, J. L., and Fraceto, L. F. (2014). Applications of controlled release systems for fungicides, herbicides, acaricides, nutrients, and plant growth hormones: a review. *Adv. Sci. Eng. Med.* 6: 373–387.
- [5]. Dipak, K. H. (2015). Recent Advancement in Pesticide Formulations for User and Environment Friendly Pest Management for users and environmental friendly pest management. *International Journal of Research and Review*. Pp 35-40.
- [6]. Doane, W. M., Shasha, B. S., Russell, C. R. (1977). Encapsulation of pesticides within a starch matrix. *ACS, Symposium series*. American Chemical Society; Washington, DC, 53; 74-83
- [7]. FAO, IFAD and WFP. (2015). The State of Food Insecurity in the World 2015. Meeting the 2015 international hunger targets: taking stock of uneven progress. Rome, FAO.
- [8]. Fontes, G.C., Calado, V.M.A., Rossi, M.A., Miguez da Rocha-Leao, M.H. (2013). Characterization of antibiotic-loaded alginate-osa starch microbeads produced by ionotropic pregelation. *Biomedicine and Biotechnology: Public Health Impact*. Volume 2013 |Article ID 472626 | 11 pages.
- [9]. Gal, E., Aires, P., Charmarro, E., and Esplugas, S., (1992). Photochemical degradation of parathion in aqueous solutions. *Water Resources Journal*
- [10]. Gomaa, H.M., Suffet, I.H. and Faust, S.D. (1969). Kinetics of hydrolysis of diazinon and dichlorvos. *Residue Review* 29:171-190
- [11]. Humpola, P.D., Odetti, H.S., Fertitta, A.E. and Vicente, J.L. (2013). Thermodynamic analysis of adsorption models of phenol in liquid phase on different activated carbons. *Journal of the Chilean chemical society*, 58(1), 1541 - 1544.
- [12]. Ihegwuagu, N. E., Sha’Ato, R., Tor-Anyiin, T. L., Nnamonu, L. A., Muller, X. and Maaza. M. (2015). Soil lixiviation and slow release pattern of starch-nano silver particles-encapsulated Dichlorvos insecticide formulation. *Journal of Agriculture and veterinary science* 8(2), p 15-24.
- [13]. Jyothi, A.N., Pillai, S.S., Aravid, M., Salim, M.A. and Kuzhilvilayil, S.J. (2018). Cassava starch-graft-poly(acrylonitrile)-coated urea fertilizer with sustained release and water retention properties. *Advances in Polymer Technology*. Volume 37, Issue 7. November 2018. Pages 2687-2694.
- [14]. Ku, Y., Chang, J-L. and Cheng, S-C. (1998). Effect of solution pH on the hydrolysis and photolysis of diazinon in aqueous solution.
- [15]. Khoiriah, K., Wellia, D.V., Gunlazuardi, J. and Safni, S. (2019). Photocatalytic degradation of commercial diazinon pesticide using C,N-codoped  $\text{TiO}_2$  as photocatalyst. *Indones. J. Chem.*, 2020, 20 (3), 587 - 596.
- [16]. Lewis, D.H. and Cowsar, D.R. (2016). Principles of controlled release pesticides ACS symposium series, American chemical society Washington D.C.
- [17]. Li, M., Tshabalala, M.A. and Buschle-Diller, G. (2015). Formulation and characterization of polysaccharide beads for controlled release of plant growth regulators. *Journal of Materials Science* 51, 4609 – 4617.
- [18]. Mogul, M.G., Akin, H., Hasirci, N., Trantolo, D.J., Gresser, J.D. and Wise, D.L. (1996) Controlled release of biologically active agents for purpose of agricultural crop management *Resources Conservation Recycling*. 16, pg 289-320.

- [19]. Moore, S. (1965). Amino acid analysis; aqueous dimethyl sulfoxide as solvent for the Ninhydrin Reaction. *Journal of Biological Chemistry* 179; 367- 388.
- [20]. Mulqueen, P. (2003) Recent advances in agrochemical formulation. *Advances in Colloid and Interface Science* 106: 83-107.
- [21]. Neri-Badang, M.C. and Chakraborty, S. (2019). Carbohydrate polymer as controlled release devices for pesticides. *Journal of Carbohydrate Chemistry*, 38; 67-85.
- [22]. Nnamonu, L.A., Nkpa, N.N., Sha'Ato, R. and Onyido, I. (2012). Adsorption and desorption studies of trifluralin on starch.
- [23]. Ogwuche, E.O., Gimba, C.E. and Abechi, E.S. (2015). An Evaluation of the Adsorptive Behaviour of Activated Carbon Derived from *HyphaeneThebaica* Nut Shells for the Removal of Dichlorvos from Wastewater. *The International Journal of Science and technology*.
- [24]. Onyido, I., Sha'Ato, R. and Nnamonu, L.A. (2012). Environmental friendly formulations of trifluralin based on alginate modified starch. *Journal of environmental protection* 3(9). 1085- 1093.
- [25]. Ouznadji, Z.B., Sahmoune, M.N. and Mezenner, N.Y. (2014). Adsorption removal of diazinon: kinetic and equilibrium study. DOI:10.1080/19443994.2014.978386.
- [26]. Ponyadira, K., Naoto M., Erni, J. and Teruo H. (2014). Mechanism of Diazinon Adsorption on iron modified montmorillonite. *American Journal of Analytical chemistry*, 5, p. 70-76.
- [27]. Sahithya, K., Devlina, D., and Nilanjana, D. (2016). Adsorption Coupled Photocatalytic Degradation of Dichlorvos Using LaNiMnO<sub>6</sub> Perovskite Nanoparticles Supported on Polypropylene Filter Cloth and Carboxymethyl Cellulose Microspheres. Published online in Wiley Online Library.
- [28]. Scher, H.B. (1999). *Controlled-release delivery systems for pesticides*. Marcel Dekker Inc., New York, CRC Press
- [29]. Shi, M., Jing, Y., Yang, L., Huang, X., Wang H., Yang, Y. and Liu, Y. (2019). Structure and Physicochemical Properties of Malate Starches from Corn, Potato and Wrinkled Pea Starches. *Polymers* **2019**, 11(9), 1523.
- [30]. Sivanantham, M. and Tata, B.V. (2012). "Swelling/deswelling of polyacrylamide gels in aqueous NaCl solution: light scattering and macroscopic swelling study," *Pramana*,
- [31]. Tiwari, A. and Bind, A. (2014). Effective Removal of Pesticide (Dichlorvos) by Adsorption onto Super Paramagnetic Poly(Styrene-co-acrylic Acid) Hydrogel from Water. *International Research Journal of Environment Sciences*, 3 (11), 41-46.
- [32]. Tovar, C.D.V., Castro, J.I., Valencia, C.H., Zapata, P.A., Solano, M.A., Lopez, E.F., Chaur, M.N., Zapata, M.E.V., Hernandez, J.H.M. (2020). Synthesis of chitosan beads incorporating graphene oxide/titanium dioxide nanoparticles or in vivo studies. *Molecules* **2020**, 25(10), 2308.
- [33]. United Nations (2014). United nations for sustainable development. [www.un.org/sustainabledevelopment/hunger](http://www.un.org/sustainabledevelopment/hunger).
- [34]. Wu, J., Lan, C. and Chan, G.Y. (2009) Organophosphorus pesticide ozonation and formation of oxon intermediates. *Chemosphere*, pp. 1308-1314.

1Okafor E.C, et. al. "Controlled Release Formulation of Dichlorvos and Diazinon Using Biocompatible Starch For Agro-Environment Sustainability." *IOSR Journal of Applied Chemistry (IOSR-JAC)*, 14(6), (2021): pp 01-09.